Journal of Sound and Vibration (2001) **240**(4), 599–612
doi:10.1006/jsvi.2000.3257, available online at http://www.idealibrary.com on IDEAL®

NON-LINEAR OSCILLATIONS OF A ROTOR IN ACTIVE MAGNETIC BEARINGS

J. C. Ji

Department of Mechanical Engineering, Baotou University of Iron and Steel Technology, Baotou 014010, *Inner Mongolia, People's Republic of China*

AND

C. H. Hansen

Department of Mechanical Engineering, The University of Adelaide, South Australia 5005, *Australia*

(*Received* 6 *December* 1999, *and in final form* 14 *June* 2000)

The non-linear response of a rotor supported by active magnetic bearings is investigated, and both primary and internal resonances are considered. The method of multiple scales is used to obtain four first order ordinary differential equations that describe the modulation of the amplitudes and phases of vibrations in the horizontal and vertical directions. The steady state response and the stability of the solutions are determined numerically from the reduced system. It is shown that the steady state solutions lose their stability by either saddle-node bifurcation or Hopf bifurcation. In the regime of multiple coexisting solutions, two stable solutions are found. The effect of imbalance eccentricity, as well as the effect of the proportional and derivative gains of the controller on the non-linear response of the system, are studied. Finally, numerical simulations are performed to verify the analytical predictions.

1. INTRODUCTION

Several components of an active magnetic bearing (AMB) are characterized by non-linear behavior and therefore the entire system is inherently non-linear [1]. However, in the simulation of the dynamic behavior of magnetically suspended rotors, the non-linearities are usually neglected for simplicity, and the components of the AMBs are modelled using linear analysis. Additionally, many of the AMB control techniques used previously are based on a linearized electro-mechanical system. In fact, the non-linear properties of AMBs can lead to a different behavior of the rotor-magnetic bearing system from that predicted by a linear model. Thus, a fundamental scientific investigation of the effects of electro-mechanical system non-linearities on the dynamic behavior of a rotor, and their influence on the performance of AMBs is required.

The effects of co-ordinate coupling, due to the geometry of the pole arrangement, on non-linear behavior have been examined in reference [2]. Multiple coexisting solutions and fractal boundaries were obtained. Stable quasi-periodic vibration has been demonstrated for large geometric coupling values for cases in which the rotor weight was neglected [3]. When the rotor weight was taken into account [4], the parameters were investigated by semi-analytical methods to find regimes of non-linear behavior such as jump phenomenon and subharmonic motion. A local bifurcation of codimension two of rotor motion was investigated on the center manifold near the double-zero degenerate point by using center

0022-460X/01/090599 + 14 $35.00/0

manifold theory and the normal form method [5]. Saddle-node bifurcation, Hopf bifurcation and saddle-connection bifurcation were found in the reduced normal form equations.

In a typical AMB, the essential non-linearity results from the force–displacement–current characteristics of the electromagnets. The non-linear magnetic forces are even more pronounced for a large air-gap AMB [6]. In this paper, a two-degree-of-freedom (d.o.f.), non-linear system, with cubic non-linearities will be used to explore the non-linear, dynamic behavior of a rotor suspended by large air gap AMBs. The fundamental resonance of the system is examined by using a perturbation method. The effects of unbalance and control gains on the steady state motion of the rotor are also investigated.

2. ROTOR–AMB SYSTEM MODEL

An AMB is shown schematically in Figure 1. The stator has eight pole pairs. For simplicity, the saturation and the hysteresis of the magnetic core material, the eddy current losses, and all other secondary effects are neglected. All magnets are assumed to have an identical structure and the same number of windings.

According to electromagnetic theory, the electromagnetic force f_i produced by every pair of electromagnets can be expressed as follows [7]:

$$f_i = \frac{1}{4}\mu_0 N^2 A \frac{I_i^2}{\delta_i^2}\cos\varphi, \quad i = 1, 2, \ldots, 8, \tag{1}$$

where μ_0 is the permeability, A is the effective cross-sectional area of one electromagnet, N is the number of windings around the core, I_i is the coil current that is equal to the sum of the bias current of the electromagnet and the control current, δ_i is the radial clearance between the stator and the rotor, and φ is the corresponding half-angle of the radial electromagnetic circuit respectively. The idealized magnetic force of equation (1) depends in a non-linear

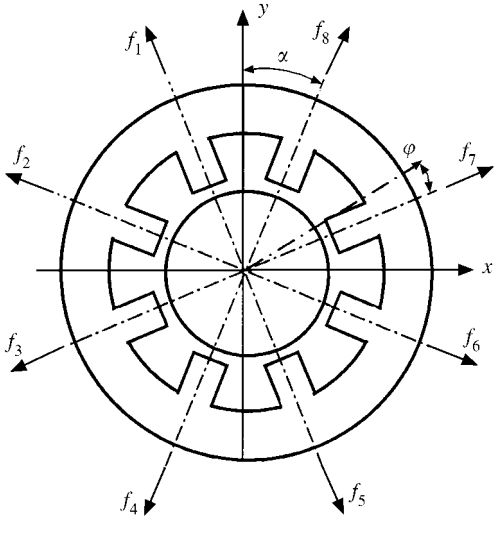

Figure 1. Schematic for modelling magnetic forces acting on the rotor.

way, on the rotor position and the current. For a large displacement or a large current, the non-linear characteristic dominates.

For an AMB, when the rotor deviation from the center of the bearings is denoted by x and y, the radial clearance between the electromagnets and the rotor can be written as

$$\begin{aligned}
\delta_i &= c_0 \pm x\sin\alpha \mp y\cos\alpha, \quad i = 1, 5,\\
\delta_i &= c_0 \pm x\sin\alpha \pm y\cos\alpha, \quad i = 4, 8,\\
\delta_i &= c_0 \pm x\cos\alpha \mp y\sin\alpha, \quad i = 2, 6,\\
\delta_i &= c_0 \pm x\cos\alpha \pm y\sin\alpha, \quad i = 3, 7,
\end{aligned} \tag{2}$$

where c_0 is the steady state air gap and α is the angle defined in Figure 1.

To reduce the non-linearity of the magnetic force and also the uncertainty of currents resulting from force changes near the zero position, the pre-magnetization current I_0 is usually sent through all coils and are superimposed on the control currents. Thus, currents flowing in the coils are given by

$$\begin{aligned}
I_1 = I_8 = I_0 - i_y, \qquad I_4 = I_5 = I_0 + i_y,\\
I_6 = I_7 = I_0 - i_x, \qquad I_2 = I_3 = I_0 + i_x.
\end{aligned} \tag{3}$$

The magnetic force acting on the rotor in each direction is the difference between the attractive forces of both magnets fixed on opposite sides. Therefore, the total electromagnetic forces in the horizontal and vertical directions are of the form

$$\begin{aligned}
f_x &= (f_6 + f_7 - f_2 - f_3)\cos\alpha + (f_5 + f_8 - f_1 - f_4)\sin\alpha,\\
f_y &= (f_1 + f_8 - f_4 - f_5)\cos\alpha + (f_2 + f_7 - f_3 - f_6)\sin\alpha.
\end{aligned} \tag{4}$$

Substituting equations (2) and (3) into equation (1), gives the resulting force as a non-linear function of the control current and the rotor displacements x and y. For small vibration amplitudes, the force, f_i, is expanded about the $(0, 0, 0)$ point using a Taylor series and is approximated by only retaining the lower order non-linear terms. The resulting expressions for the electromagnetic forces from all magnets acting together can be derived from equation (4) as

$$\begin{aligned}
f_x &= f_x(linear) + f_x(cubic) + 0(4),\\
f_y &= f_y(linear) + f_y(cubic) + 0(4),
\end{aligned} \tag{5}$$

where $0(4)$ denotes terms of order greater than four. Here, for the sake of brevity, the simple notations $f_x(linear)$ and $f_y(linear)$ are used to denote the linear terms, while $f_x(cubic)$ and $f_y(cubic)$ represent the cubic non-linear terms respectively.

For magnetically suspended rotors various control techniques have been used to achieve various aims. However, in this article, only the current PD controller is considered:

$$i_x = k_p x + k_d \dot{x}, \qquad i_y = k_p y + k_d \dot{y}, \tag{6}$$

where k_p is the proportional gain and k_d is the derivative control constant, and the PD gains of the controllers, for all eight pole pairs are taken to be same.

As the focus of the work is on the effect of non-linearity of AMBs on the non-linear response of a rotor, the rotor is assumed, for simplicity, to be a rigid body supported in AMBs. Thus, the model consists of one mass with two degrees of freedom. The equations of motion governing the unbalance of the rotor can be written as

$$m\ddot{x} = f_x - c\dot{x} + me\Omega^2 \cos \Omega t, \qquad m\ddot{y} = f_y - c\dot{y} + me\Omega^2 \sin \Omega t, \tag{7}$$

where m, e, c, Ω are the mass, the eccentricity of unbalance, the damping coefficient, and the rotor speed respectively. The rotor weight is neglected in the present analysis. If the rotor weight is taken into account, the resulting total electromagnetic forces will be expressed in different forms. This is the subject of work currently in progress.

Substituting equations (5) and (6) into equation (7), introducing non-dimensional parameters $x = c_0\bar{x}$, $y = c_0\bar{y}$, $i_x = I_0\bar{i}_x$, $i_y = I_0\bar{i}_y$, $t = B\bar{t}$, $\Omega = B^{-1}\bar{\Omega}$, and omitting the hat for brevity, equation (7) can be rearranged as

$$\ddot{x} + 2\mu\dot{x} + \omega^2 x - (\alpha_1 x^3 + \alpha_2 xy^2 + \alpha_3 x^2\dot{x} + \alpha_4\dot{x}y^2 + \alpha_5 x\dot{y}^2 + \alpha_6 x\dot{x}^2 + \alpha_7 xy\dot{y}) = 2f\cos \Omega t,$$

$$\ddot{y} + 2\mu\dot{y} + \omega^2 y - (\alpha_1 y^3 + \alpha_2 x^2 y + \alpha_3 y^2\dot{y} + \alpha_4 x^2\dot{y} + \alpha_5\dot{x}^2 y + \alpha_6 y\dot{y}^2 + \alpha_7 x\dot{x}y) = 2f\sin \Omega t, \tag{8}$$

where μ, ω, Ω, f and the coefficients of the non-linear terms, α_i, are defined in Appendix A. The closed form of the solutions of equation (8) cannot be found. Hence, approximate solutions will be sought by using the method of multiple scales (MMS) [8].

3. PERTURBATION ANALYSIS BY USING MMS

The MMS [8] is employed to obtain four first order amplitude– and phase–modulated equations. To achieve this, the small dimensionless parameter, ε, is introduced as a book-keeping device to indicate the smallness of damping (derivative gain), non-linearities and excitation (unbalance). Assuming the amplitude of motion is small, equation (8) can be expressed as

$$\ddot{x} + \varepsilon 2\mu\dot{x} + \omega^2 x - \varepsilon(\alpha_1 x^3 + \alpha_2 xy^2 + \alpha_3 x^2\dot{x} + \alpha_4\dot{x}y^2 + \alpha_5 x\dot{y}^2 + \alpha_6 x\dot{x}^2 + \alpha_7 xy\dot{y})$$
$$= \varepsilon 2f\cos \Omega t,$$

$$\ddot{y} + \varepsilon 2\mu\dot{y} + \omega^2 y - \varepsilon(\alpha_1 y^3 + \alpha_2 x^2 y + \alpha_3 y^2\dot{y} + \alpha_4 x^2\dot{y} + \alpha_5\dot{x}^2 y + \alpha_6 y\dot{y}^2 + \alpha_7 x\dot{x}y)$$
$$= \varepsilon 2f\sin \Omega t, \tag{9}$$

where $|\varepsilon| \ll 1$, $x = \varepsilon^{\frac{1}{2}}\bar{x}$, $y = \varepsilon^{\frac{1}{2}}\bar{y}$, $\mu = \bar{\mu}\varepsilon^{-1}$, $2\varepsilon\bar{f} = 2f\varepsilon^{-\frac{1}{2}}$. Here, for the sake of brevity, the "overbar" has been omitted.

Equation (9) is a two-degree-of-freedom non-linear system with cubic non-linearities. Obviously, the system is in a one-to-one internal resonance condition, because its linearized natural frequencies are equal. When the natural frequencies and forcing frequency satisfy certain external resonance conditions, different types of external resonance such as fundamental, subharmonic and superharmonic resonance can occur. Here, the fundamental resonance is analyzed. To study the fundamental resonance, the frequency of the external

excitation is assumed to be almost equal to the linearized natural frequencies. To describe this proximity, the external detuning parameter, σ, is introduced as

$$\omega^2 = \Omega^2 + \varepsilon\sigma. \tag{10}$$

By using the MMS, the following first order approximation for the solutions of equation (9) are obtained:

$$x = a_1 \cos(\Omega t + \beta_1), \qquad y = a_2 \cos(\Omega t + \beta_2). \tag{11}$$

The amplitudes, a_i, and phases, β_i, of the fundamental resonance response are governed by

$$\begin{aligned}
a_1' &= -\mu a_1 + b_1 a_1 a_2^2 \sin 2\phi + b_2 a_1^3 + b_3 a_1 a_2^2 \cos 2\phi + b_4 a_1 a_2^2 - f_1 \sin\beta_1,\\
a_1\beta_1' &= \sigma_1 a_1 - b_5 a_1^3 - b_6 a_1 a_2^2 - b_1 a_1 a_2^2 \cos 2\phi + b_3 a_1 a_2^2 \sin 2\phi - f_1 \cos\beta_1,\\
a_2' &= -\mu a_2 - b_1 a_1^2 a_2 \sin 2\phi + b_2 a_2^3 + b_3 a_1^2 a_2 \cos 2\phi + b_4 a_1^2 a_2 - f_1 \cos\beta_2,\\
a_2\beta_2' &= \sigma_1 a_2 - b_5 a_2^3 - b_6 a_1^2 a_2 - b_1 a_1^2 a_2 \cos 2\phi - b_3 a_1^2 a_2 \sin 2\phi + f_1 \sin\beta_2,
\end{aligned} \tag{12}$$

where $\phi = \beta_2 - \beta_1$, and the coefficients σ_1, f_1 and b_i $(i = 1, 6)$ are defined in Appendix B.

For the steady state response, $a_{1,2}' = 0$ and $\beta_{1,2}' = 0$. Equation (12) can then be reduced to a set of four non-linear algebraic equations, and the steady state response obtained from these four algebraic equations by using the Newton–Raphson procedure. The stability of steady state solutions can be examined by computing the eigenvalues of the coefficient matrix of characteristic equations, which are derived from equation (12) in terms of small disturbances to the steady state solutions.

4. NUMERICAL RESULTS AND DISCUSSION

In this section, the steady state responses of the system are investigated extensively for different system parameters under primary and internal resonance. It is shown that the steady state response loses its stability either by saddle node (SN) or by Hopf bifurcation (HB). In the region of multiple coexisting solutions, two stable solutions exist, and the initial conditions determine which curve is followed. The fixed points of the four non-linear algebraic equations reduced from system (12) correspond to the periodic responses of the original system (8). The four non-linear algebraic equations are numerically solved by the Newton–Raphson procedure. The stability of the steady state response is obtained from the eigenvalues of the corresponding Jacobian matrix. Moreover, to verify the analytical predictions, equation (8) is numerically integrated with a fourth order Runge–Kutta algorithm. In the frequency and forced response plots the stable and unstable branches are indicated, respectively, by solid and dot broken lines.

The modal amplitudes, a_1 and a_2, of the periodic solutions are shown in Figure 2 as functions of the forcing amplitude, f_1. To perform the numerical simulations, the values for the system parameters are chosen as follows: $\Omega = 1$, $\alpha = 0{\cdot}3926991$, $c_1 = 0{\cdot}001$, $p = 1{\cdot}22$, $d = 0{\cdot}005$. It can be seen that the response curves of the two modal amplitudes are similar and topologically equivalent. There are three types of solutions. One corresponds to equal

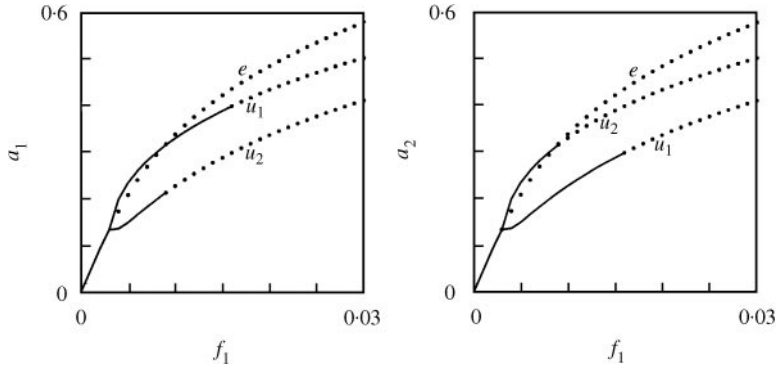

Figure 2. The response amplitudes a_1 and a_2 as a function of the forced amplitude for positive external detuning, under $p = 1{\cdot}22$, $d = 0{\cdot}005$.

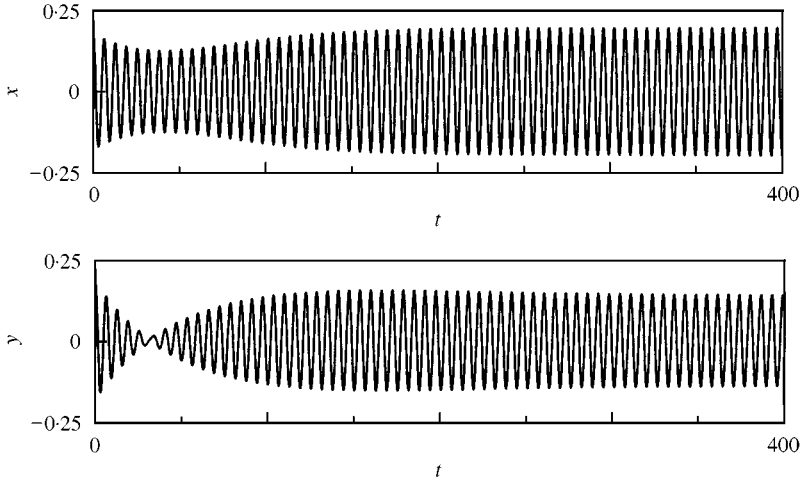

Figure 3. Transition from an unstable steady state motion to a stable one under $p = 1{\cdot}22$, $d = 0{\cdot}005$, $f_1 = 0{\cdot}004$, with initial conditions $x(0) = 0{\cdot}18$, $y(0) = 0{\cdot}18$ and zero initial velocities.

amplitudes of primary resonance responses for the two directions, $a_1 = a_2$, which is illustrated by the curve titled, "e", in the figure. The other two correspond to different amplitudes, $a_1 > a_2$, and $a_1 < a_2$, which are represented by the curves labelled "u1" and "u2" respectively.

When the forcing amplitude is small, the system admits a stable solution with equal amplitudes of response, $a_1 = a_2$. This stable solution loses its stability via SN bifurcation at $f_1 = 0{\cdot}003$, and a jump from this unstable steady motion to a stable one occurs. In Figure 3, a jump from an unstable steady motion to a stable one is illustrated. The numerical simulation was done using $f_1 = 0{\cdot}004$, initial conditions $x(0) = 0{\cdot}18$, $y(0) = 0{\cdot}18$ and zero initial velocities (corresponding to an unstable solution), while other parameters are the same as those used to derive Figure 2. It can be seen that after some initial transients, the motion settles down to the theoretically predicted stable steady state response, which corresponds to the stable part of branch "u1" of Figure 2.

As $f_1 > 0{\cdot}003$, a total of three solutions exist, but only two stable branches occur. The solution for which $a_1 = a_2$ is an unstable one, while the solutions corresponding to unequal amplitudes are stable.

As the amplitude of excitation is varied, the two stable branches lose their stability by HB occurring at $f_1 = 0{\cdot}009$ and $0{\cdot}016$, respectively, and amplitude-modulated motion is generated. The existence of the HB is detected by examining the eigenvalues of the matrix of the coefficients of the variational equations, evaluated for the steady state solutions. Such an examination shows a pair of complex eigenvalues passing through the imaginary axis, which gives rise to HB. The HB is expected to lead to amplitude modulation of the steady state response. The prediction will shortly be verified by numerically integrating the system equation (8).

In a typical linear dynamic system, the steady state amplitude is independent of initial conditions; that is, the response is unique. This is not necessarily the case for non-linear systems. For a forced non-linear system, when two or more stable steady state solutions exist, the initial conditions determine which steady state solution is picked up. It may be noted that there exist two stable solutions in the interval between $f_1 = 0{\cdot}003$ and $0{\cdot}009$, the physically attainable solution is determined by the initial conditions. Figures 4(a) and 4(b)

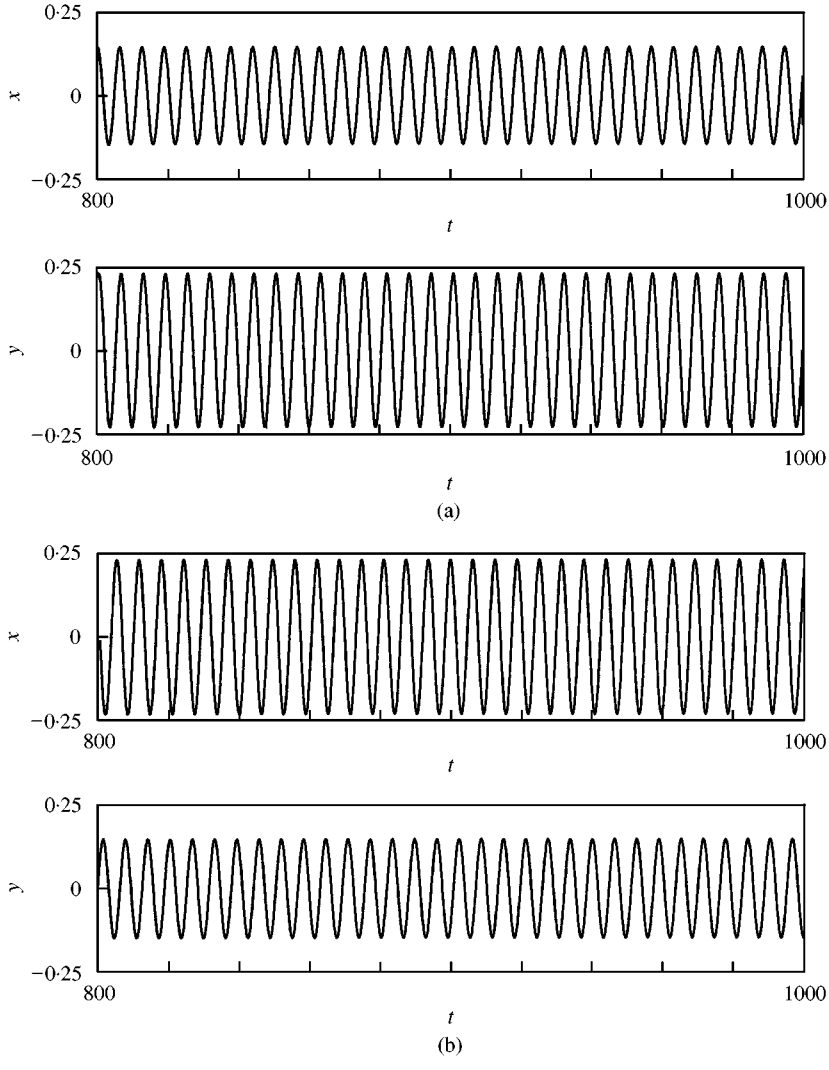

Figure 4. Continued.

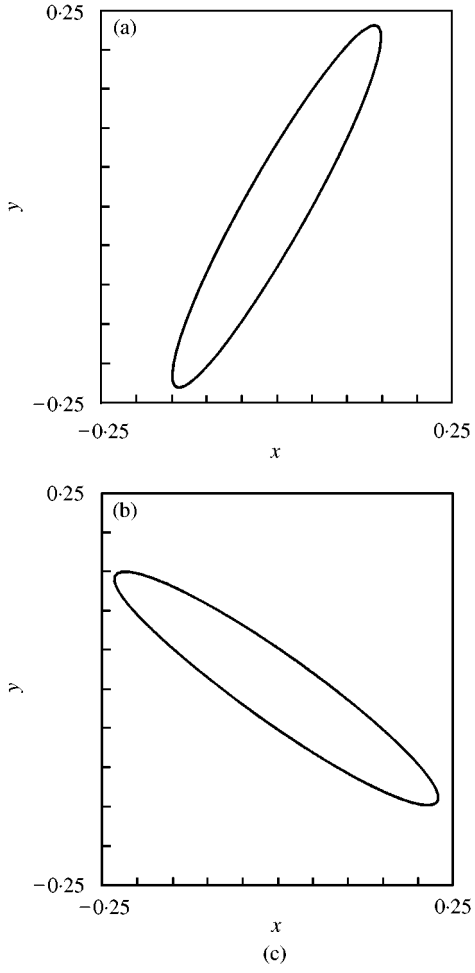

Figure 4. Periodic motions of the system under $p = 1{\cdot}22$, $d = 0{\cdot}005$, $f_1 = 0{\cdot}005$. (a) Response of system corresponds to branch "u2" of Figure 2; (b) Response of system corresponds to branch "u1" of Figure 2; (c) The corresponding orbit of the rotor.

show the steady state response of the system for $f_1 = 0{\cdot}005$, corresponding to branches "u1" and "u2" respectively. As the initial conditions are different, the steady state solutions are different. The initial conditions for computing these responses are chosen as $x(0) = 0{\cdot}0206$, $\dot{x}(0) = 0{\cdot}1164$, $y(0) = -0{\cdot}1166$ and $\dot{y}(0) = 0{\cdot}0184$ for Figure 4(a), while $x(0) = 0{\cdot}1196$, $\dot{x}(0) = 0{\cdot}1943$, $y(0) = -0{\cdot}1198$ and $\dot{y}(0) = -0{\cdot}0839$ for Figure 4(b). From this example it can be seen that the results of numerical integration agree well with the analytical predictions.

If, however, the cosine and sine parts of the force are exchanged, the solutions for the x and y directions exchange places. This dependence on phase or initial conditions is a characteristic of a non-linear system. The coexistence of multiple solutions and the dependence on initial conditions are an important challenge in the controller design.

An interesting feature of the system is found for the forced case corresponding to Figure 2. Suppose that the system is started from each of two stable branches separately. With an increase in forced excitation, the response of the system will be totally different in each case, as illustrated in Figures 5 and 6, which show the amplitude-modulated motions for

$f_1 = 0{\cdot}021$ and $0{\cdot}030$ respectively. Once again, this indicates that the response is dependent on the initial conditions, even for the amplitude-modulated response.

As the linearized natural frequencies of the system are related to the proportional gain (see Appendix A), the external detuning shown in Figure 2 is positive. For the case of negative external detuning, the variation of response amplitudes as a function of the forced amplitude is shown in Figure 7. The values of the system parameters are chosen to be same as those of Figure 2 except for the proportional gain. By comparing these two figures, it can be seen that they are topologically equivalent. The major difference is that the region of amplitude of excitation for existence of stable solutions for a negative detuning is shorter than that for a positive detuning. The values of the amplitude of excitation are decreased from $f_1 = 0{\cdot}003$ to $0{\cdot}002$ for SN bifurcation, and from $f_1 = 0{\cdot}009$ and $0{\cdot}016$ to $f_1 = 0{\cdot}006$ and $0{\cdot}009$ for HB respectively.

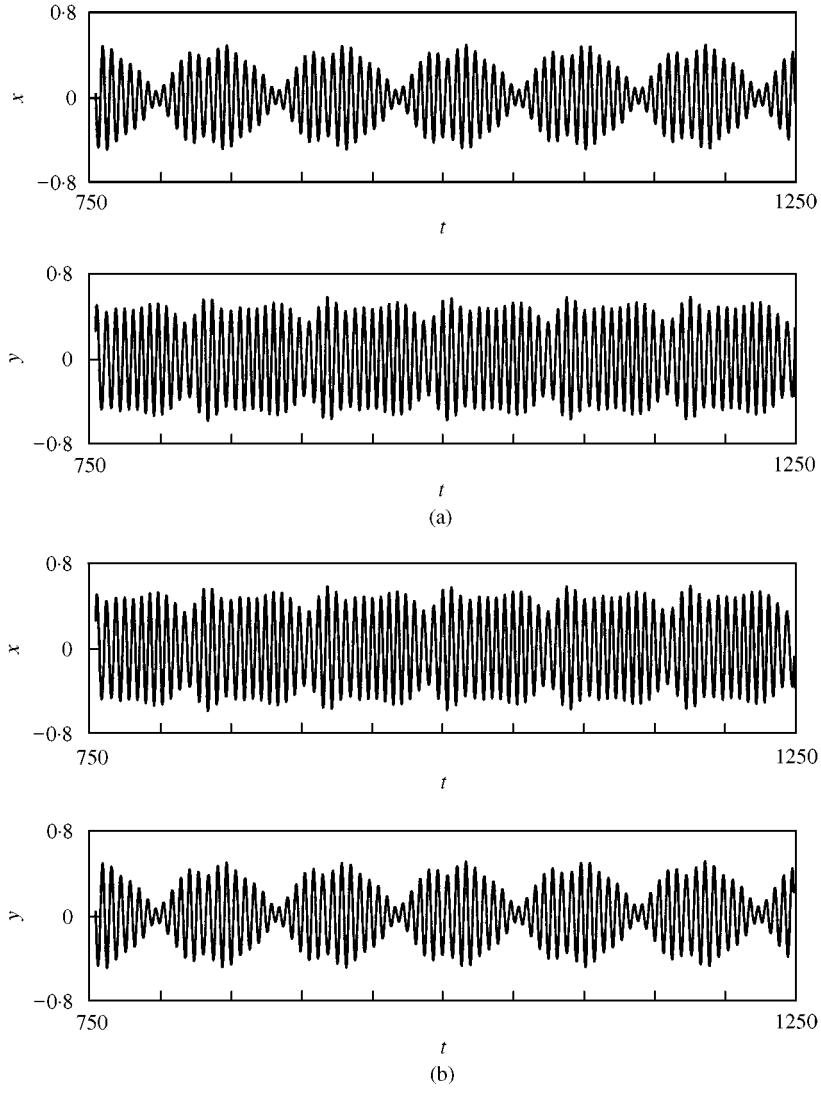

Figure 5. Continued.

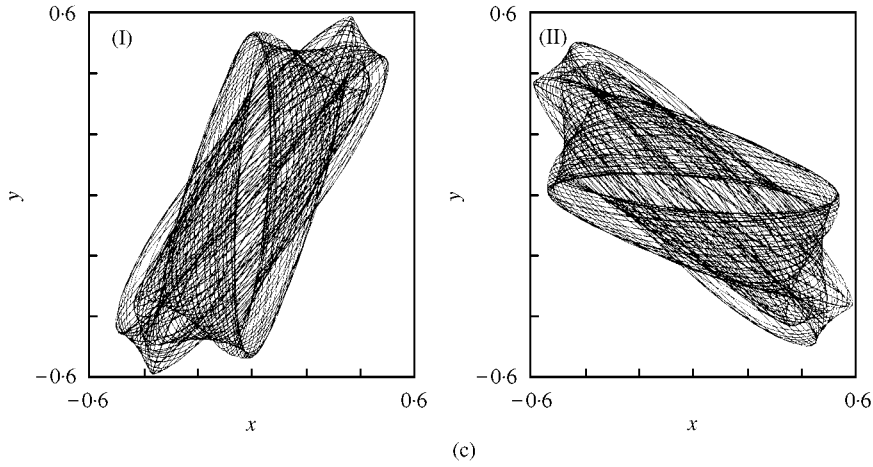

Figure 5. Amplitude-modulated motions under $p = 1{\cdot}22, d = 0{\cdot}005, f_1 = 0{\cdot}021$. (a) Forced response corresponding to branch "u2" of Figure 2; (b) Forced response corresponding to the branch "u1" of Figure 2; (c) The corresponding orbit of the rotor.

Figure 8 shows the response amplitudes as a function of forced amplitude for a lower value of derivative gain. The values of all parameters except the derivative gain are equal to those for the case shown in Figure 7. It can be observed that with a lower value of derivative constant, the critical points for SN and HB shift to the left. The regime of amplitude of excitation for existence of stable steady state motion is narrower too.

Keeping other system parameters constant, with $f_1 = 0{\cdot}008$, $d = 0{\cdot}005$, and $c_1 = 0{\cdot}001$, the effect of proportional gain on the response amplitudes is shown in Figure 9. There are three coexisting solutions. The solution with equal amplitudes is unstable. The other two solutions with unequal amplitudes lose their stability via HB. There also exists an interval of two coexisting stable solutions. With an increase in proportional gain, the stable branch of the response, $a_1 > a_2$, increases until it reaches the critical point. The amplitude of response, a_2, increases more sharply than a_1 does.

The effect of the derivative gains on the response amplitudes can also be examined. Figure 10 shows the influence of increasing the value of the derivative gain while the proportional gain is held constant at 1·215. The values of all parameters except the proportional gain are equal to those for the case shown in Figure 9. With an increase in the derivative control constant, the response amplitudes of unstable and stable branches decrease. It is easy to see that the derivative gain can suppress the vibration, but cannot eliminate the number of solutions.

5. CONCLUSIONS

The non-linear response of a rotor in active magnetic bearings (AMBs) has been investigated, and both fundamental and internal resonance conditions have been considered. It has been shown that the non-linear properties of AMBs can lead to phenomena that are not described by a linear model, indicating the importance of taking non-linearities into account.

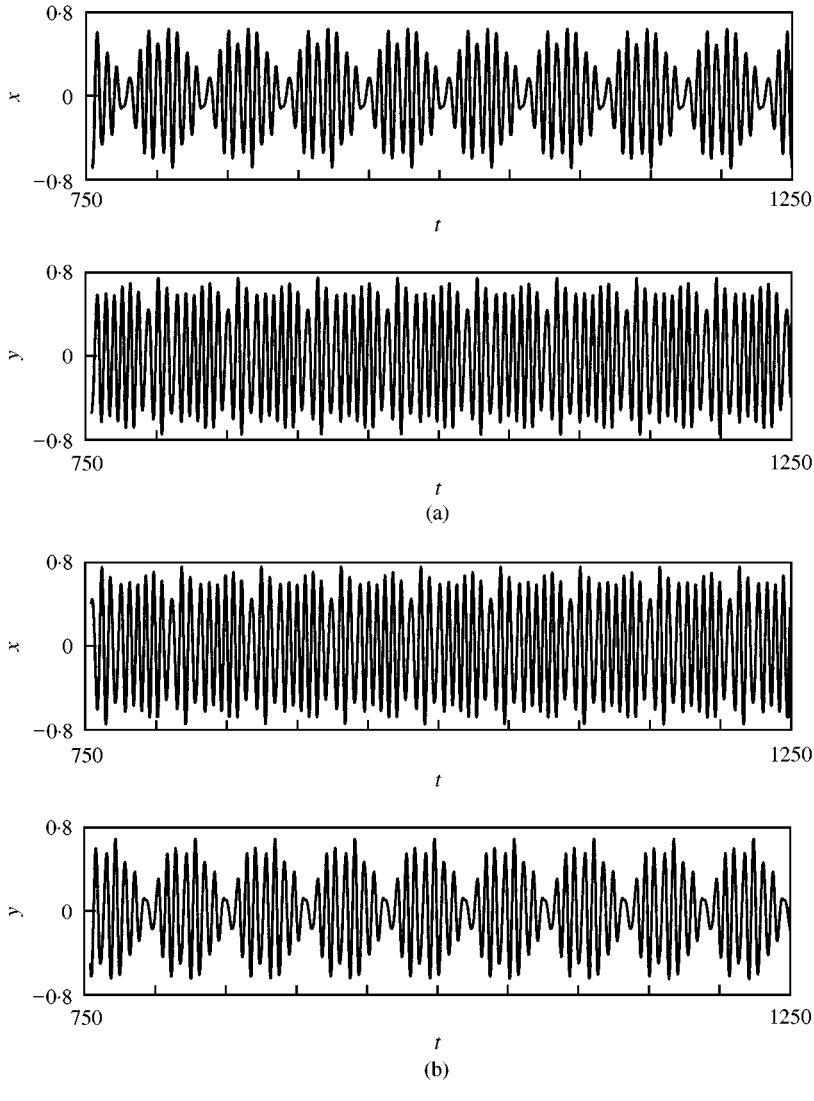

Figure 6. Continued.

The rotor-AMB dynamic system exhibits a variety of interesting phenomena, including bifurcation, jump, sensitivity to initial conditions, coexistence of multiple solutions, and amplitude-modulated motions. The method of multiple scales (MMS) has been used to determine the four first order averaged equations. The stability and bifurcation of the forced response are studied for various system parameters. It has been shown that the solutions corresponding to equal amplitudes for the x and y directions lose their stability via SN bifurcation. The responses with unequal amplitudes lose their stability through HB and then amplitude-modulated motions are generated. The results obtained by the perturbation method and by numerical integration are in good agreement. The results presented are expected to be useful in the design of a controller to reduce the vibration amplitude of rotor-AMB systems.

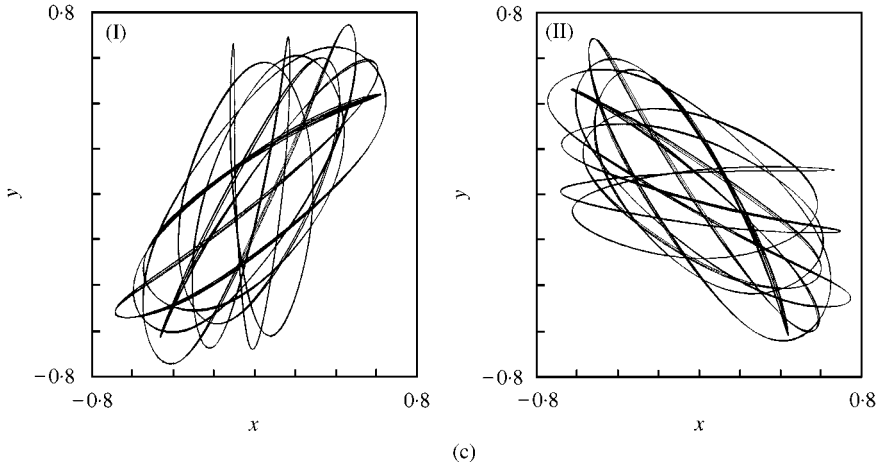

Figure 6. Amplitude-modulated motions under $p = 1{\cdot}22, d = 0{\cdot}005, f_1 = 0{\cdot}030$. (a) Forced response corresponding to branch "u2" of Figure 2; (b) Forced response corresponding to branch "u1" of Figure 2; (c) The corresponding orbit of the rotor.

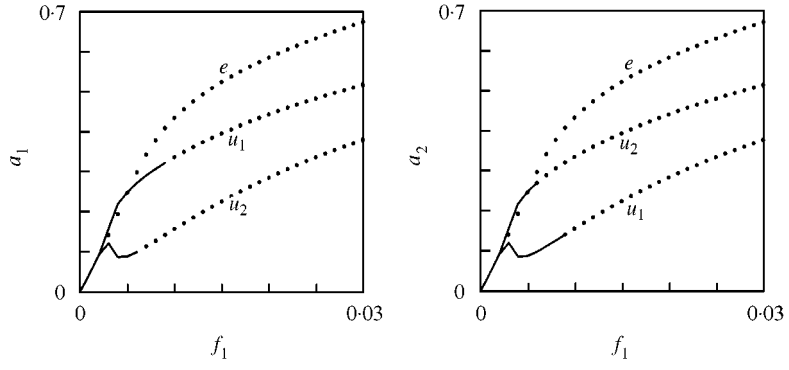

Figure 7. The response amplitudes a_1 and a_2 as a function of the forced amplitude for negative external detuning under $p = 1{\cdot}215, d = 0{\cdot}005$.

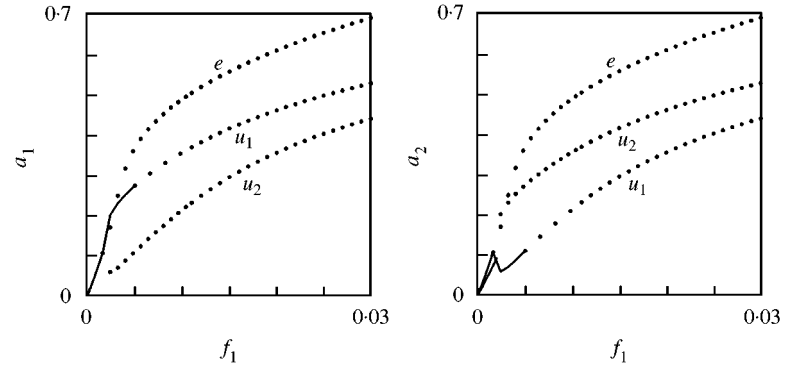

Figure 8. The response amplitudes a_1 and a_2 as a function of the forced amplitude for negative external detuning under $p = 1{\cdot}215, d = 0{\cdot}003$.

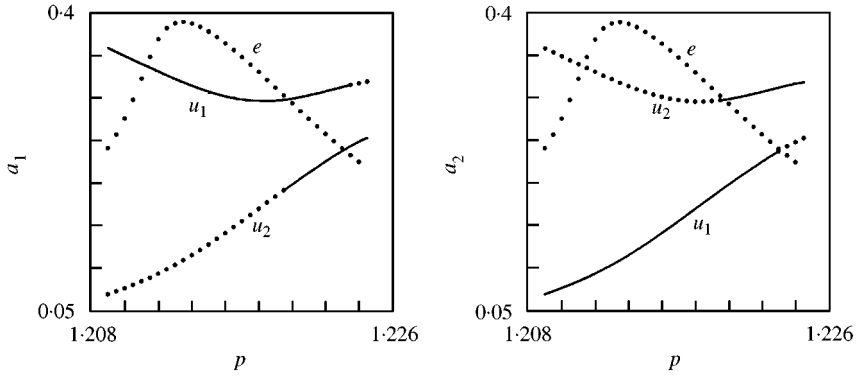

Figure 9. The response amplitudes a_1 and a_2 as a function of the dimensionless proportional gain for $f_1 = 0{\cdot}008$, $d = 0{\cdot}005$.

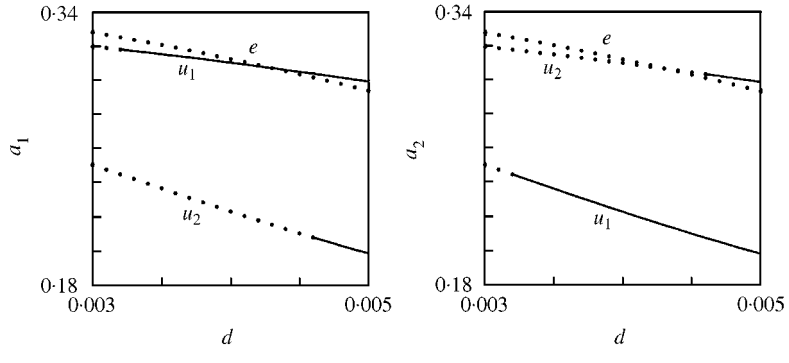

Figure 10. The variation of derivative gain on the response amplitude for positive external detuning, under $p = 1{\cdot}22$, $f_1 = 0{\cdot}008$.

ACKNOWLEDGMENT

This research was supported in part by the Key Project Foundation of Educational Committee of Inner Mongolia and by the Natural Science Foundation of Inner Mongolia.

REFERENCES

1. G. SCHWEITZER, A. TRAXLER and H. BLEULER 1993 *Magnetlager*. Berlin, Herdelberg, New York: Springer-Verlag.
2. L. N. VIRGIN, T. F. WALSH and J. D. KNIGHT 1995 *American Society of Mechanical Engineers, Journal of Engineering for Gas and Turbines and Power* **117**, 582–588. Non-linear behavior of a magnetic bearing system.
3. M. CHINTA, A. B. PALAZZOLO and A. KASCAK 1996 *Proceedings of 5th International Symposium on Magnetic Bearings*, Kanazawa, Japan, 147–152. Quasiperiodic vibration of a rotor in a magnetic bearing with geometric coupling.
4. M. CHINTA and A. B. PALAZZOLO 1998 *Journal of Sound and Vibration* **214**, 793–803. Stability and bifurcation of rotor motion in a magnetic bearing.
5. J. C. JI, L. YU and A. Y. T. LEUNG 2000 *Journal of Sound and Vibration* **235**, 133–151. Bifurcation behavior of a rotor in active magnetic bearings.

6. M. S. DE QUEIROZ, D. M. DAWSON and A. SURI 1998 *IEE Proceedings Control Theory and Applications* **145**, 269–276. Nonlinear control of a large-gap 2-DOF magnetic bearing system based on a coupled force model.
7. D. LAIER and R. MARKERT 1995 *Proceedings of the* 1*st Conference on Engineering Computation and Computer Simulation ECCS*-1, *Changsha*, *China*, Vol. I, 473–482. Simulation of nonlinear effects on magnetically suspended rotors.
8. A. H. NAYFEH 1973 *Perturbation Methods*. New York: Wiley–Interscience.

APPENDIX A

Expressions for the coefficients of equation (8):

$$p = \frac{k_p c_0}{I_0}, \qquad d = \frac{k_d c_0}{I_0 B}, \qquad B^2 = \frac{4mc_0^3}{\mu_0 N^2 A I_0^2}, \qquad c_1 = \frac{cc_0}{B},$$

$$2\mu = 8d\cos\alpha + c_1,$$

$$\omega^2 = 8(p\cos\alpha - 1),$$

$$\alpha_1 = 16(\cos^4\alpha + \sin^4\alpha) - 24p\cos^3\alpha + 8p^2\cos^2\alpha,$$

$$\alpha_2 = 96\cos^2\alpha\sin^2\alpha - 72p\cos\alpha\sin^2\alpha + 8p^2\sin^2\alpha,$$

$$\alpha_3 = -24d\cos^3\alpha + 16pd\cos^2\alpha,$$

$$\alpha_4 = -24d\cos\alpha\sin^2\alpha,$$

$$\alpha_5 = 8d^2\sin^2\alpha,$$

$$\alpha_6 = 8d^2\cos^2\alpha,$$

$$\alpha_7 = 16pd\sin^2\alpha - 48d\sin^2\alpha\cos\alpha.$$

APPENDIX B

Expressions for the coefficients of equation (12):

$$b_1 = \frac{1}{8\Omega}(\alpha_2 - \Omega^2\alpha_5), \quad b_2 = \tfrac{1}{8}\alpha_3, \quad b_3 = \tfrac{1}{8}(\alpha_7 - \alpha_4), \quad b_4 = \tfrac{2}{8}\alpha_4,$$

$$b_5 = \frac{1}{8\Omega}(3\alpha_1 + \Omega^2\alpha_6), \quad b_6 = \frac{1}{8\Omega}(2\alpha_2 + 2\Omega^2\alpha_5), \quad \sigma_1 = \frac{\sigma}{2\Omega}, \quad f_1 = \frac{f}{\Omega}.$$